

Resonance line polarization in the presence of wave motion

K.E. Rangarajan

Indian Institute of Astrophysics Bangalore 560 034, India (rangaraj at iiap.ernet.in)

Received 27 November 1995 / Accepted 19 September 1996

Abstract. The effect of wave velocity on resonance line polarization is studied. We assumed a photosphere - chromosphere type of temperature structure for the atmosphere with plane parallel symmetry. The "Discrete Space Theory technique" to solve the polarized radiative transfer in the presence of velocity fields and under the assumption of Complete Redistribution mechanism is briefly described along with the numerical checks performed. We considered both sinusoidal and sawtooth wave functions for the velocity in the medium. We find the linear polarization in the resonance lines to be increased when averaged over the whole period of the wave compared to the static medium case. The sawtooth wave shows a different average polarization profile compared to the sinusoidal wave. Line center intensity as well as the polarization vary with a period which is half of that of the wave. The variation amplitude for polarization is higher compared to the intensity towards the limb. Hence polarization in the limb may serve as an additional useful information to characterize the wave.

Key words: Sun: atmosphere – stars: atmospheres – polarization – radiative transfer – waves

1. Introduction

The study of waves and wave motion in the solar atmosphere has played an important role in identifying the heating mechanisms of chromosphere and corona. Phase relations between velocity and brightness fluctuations observed in spectral lines in the visible are utilized both to diagnose the dynamical state of the solar atmosphere and to examine the various oscillatory motions (Deubner, 1991). Fluctuations in the resonance line polarization in the presence of acoustic wave may provide additional information on the characteristics of waves. In this paper we study the time evolution of resonance line polarization in the presence of wave motions. In the following paragraphs we give a brief outline of the observations and the theory of resonance line polarization pertaining to the study of solar atmosphere. A partial list of the existing literature on the calculations of the resonance line intensity profiles in the presence of wave motion is also described.

1.1. Resonance line polarization in the solar atmosphere

Ever since Redman (1941) observed the Ca I resonance polarization, this topic has received considerable attention. The observed polarization along with the relevant theory has been used to study the solar atmosphere. Stenflo et al. (1983 a,b) has published an extensive survey of linear polarization covering the wavelength range 3165Å to 9950Å and has found a variety of effects due to resonance scattering. A detailed investigation of nonmagnetic scattering polarization in the Ca I 4227Å resonance line was made by Dumont et al (1973). Rees and Saliba (1982) pointed out that the partial frequency redistribution which is known to play an important role in the formation of strong resonance lines is responsible for the wing maximum in the observed polarization. Faurobert - Scholl has studied this phenomenon in a series of papers over the last few years. She has successfully applied the theory of Hanle effect on resonance line polarization to derive the weak magnetic field strength and Van der Waal broadening constant (Faurobert - Scholl, 1992, Faurobert - Scholl et al 1995) in the solar atmosphere. Mohan Rao and Rangarajan (1993) considered the effect of collisional redistribution on resonance line polarization and showed that the percentage of polarization at the line center is a monotonic function of the coherence parameter γ when depolarizing collisions are included in the calculations. Recently, Stenflo (1994) has discussed the diagnostic value of the resonance line polarization in an exhaustive volume.

1.2. Study of wave motion on resonance lines

Cram (1972) has attempted to reproduce the observed asymmetries and the wavelength shifts of the central absorption of Ca II H and K lines by considering the effects of vertical velocity fields in the solar atmosphere. Shine (1975) has investigated the influence of mesoscale velocity fields upon the line profiles. He employed the periodic and undamped sinusoidal and sawtooth wave functions to represent the velocity. He could obtain asymmetric time averaged line profiles when a sawtooth type of wave is present. We have used the same type of undamped periodic waves in this study. Heasley (1975) made a theoretical study of the influence of propagating acoustic pulses in the solar chromosphere upon the Ca II resonance line profiles. Scharmer (1984)

made a time series calculations of the line profiles affected by a propagating wave. He chose the atmospheric structure and parameters in such a way that it represents roughly the conditions of Ca II K line in a chromosphere. The calculations were made to mimic the evolution of the Ca II K line when an acoustic wave propagates through the atmosphere. The wave chosen was a damped one with a sinusoidal function representing the velocity. He obtained measurable differences in the time average intensity profile compared to the one produced by a static atmosphere. He found the line center intensity to vary with a period which is half of that of the wave. A numerical method developed by Scharmer and Nordlund (1982) to solve the transfer equation was demonstrated by his application. We have also taken the same model and obtained similar results for the intensity by our method. Rammacher and Ulmschneider (1992) have shown that short period acoustic waves can generate 3 min. type phenomena and that they are able to produce a core evolution pattern very similar to that of the observed Ca II K_{2v} cell grains. Using these waves in their calculations, they were able to account for the $K_{2v} - K_{2r}$ asymmetry, the K_3 Doppler evolution and the symmetric wing brightening behaviour. The influence of MHD waves on circular polarization was investigated by Solanki and Roberts (1992). For propagating waves they find that with an appropriate choice of spectral lines, a lower limit on the transported energy can be set up by observing the zero - crossing wavelength of Stokes V, while an upper limit can be derived from the line widths. They have also stressed the importance of radiative transfer effects.

1.3. Aim of this study

All the existing calculations with wave (acoustic) motions have so far been performed for obtaining the specific intensity. But now with the advent of fast detectors like CCD etc we may be able to observe resonance line polarization profiles with a fine time resolution. Such observations may give some additional clues to the nature of the velocity fields present in the sun. Therefore we have decided to perform the resonance line polarization calculations taking into account of the velocity fields.

2. Polarized line transfer equation and the method of solution

In a non magnetic plane-parallel atmosphere with azimuthal symmetry in the radiation field, it is sufficient to consider the Stokes parameters I_l and I_r to represent the polarization state of the radiation field. The total intensity is defined as $I = I_l + I_r$ and the Stokes Q parameter is defined as $Q = I_l - I_r$. As in Chandrasekhar(1960), I_l and I_r denote the intensities of linearly polarized radiation along two perpendicular directions l and r . The linear polarization is defined as $p = (Q/I)$. With the above definitions, the vector transfer equation for a two-level atom becomes

$$\mu \frac{d\mathbf{I}(x, \mu, z)}{dz} = -\chi(x, \mu, z) \mathbf{I}(x, \mu, z) + \boldsymbol{\eta}(x, \mu, z), \quad (1)$$

Here $\mathbf{I} = (I_l, I_r)^T$ and $\boldsymbol{\eta}$ is the emission coefficient. The total absorption coefficient is given by

$$\chi(x, \mu, z) = \chi_l(z) \phi(x, \mu, z) + \chi_c(x, \mu, z). \quad (2)$$

The optical depth scale is defined as $d\tau(z) = -\chi_l(z)dz$. The symbol μ denotes $\cos(\theta)$ where θ is the angle made by the ray with the normal to the surface. It is convenient to measure the frequency displacements from the line center in units of Doppler width $\Delta\nu_D = \nu_0 v_{th}/c$, where v_{th} is the thermal velocity. Any other velocity, say V , is also measured in thermal velocity unit. Then the transformation between observer's frame and atom's frame frequency is given by (Mihalas, 1978)

$$x' = x - \mu V \quad (3)$$

where

$$x = \frac{\nu - \nu_0}{\Delta\nu_D}, \quad \text{with } \Delta\nu_D = \frac{\nu_0}{c} \sqrt{\frac{2kT}{M}}. \quad (4)$$

In Eq.(2), χ_c and χ_l are the coefficients of continuous absorption and atomic absorption at the line center respectively. ν_0 is the line center frequency. The constants c and k are the velocity of light and Boltzmann constant. M is the mass of the atom under consideration. We have used Voigt function with a depth independent damping parameter as the absorption profile throughout this study. In the presence of velocity the profile function is given by,

$$\phi(x, \mu, z) \equiv \phi(x - \mu V; z). \quad (5)$$

All the other quantities have their usual meaning. The total source function $\mathbf{S}_{tot}(x, \mu, z)$ is given by

$$\mathbf{S}_{tot}(x, \mu, z) = \frac{\phi(x, \mu) \mathbf{S}_L(x, \mu, z) + \beta_c \mathbf{S}_C}{\phi(x, \mu) + \beta_c}, \quad (6)$$

where $\beta_c = \chi_c/\chi_l$ and continuum source function \mathbf{S}_C is defined as

$$\mathbf{S}_C = \frac{1}{2} B(x) \mathbf{1} = \frac{1}{2} B \mathbf{1}; \quad \mathbf{1} = [1 \ 1]^T, \quad (7)$$

where B is the Planck function. We have considered only the complete redistribution mechanism which may be valid in the Doppler core of the line. The implication of this assumption is discussed in the next section. In the absence of magnetic field and for the s - p - s transition (intrinsic depolarization is absent), the line source function for the complete redistribution mechanism becomes,

$$\mathbf{S}_L(x, \mu, z) = \frac{(1 - \epsilon)}{2} \int_{-\infty}^{+\infty} dx'' \int_{-1}^1 \mathbf{P}_R(\mu, \mu') \times \times \mathbf{I}(x'', \mu', z) \phi(x'', \mu') d\mu' + \frac{\epsilon}{2} B \mathbf{1}, \quad (8)$$

where \mathbf{P}_R is the Rayleigh scattering phase matrix defined by Chandrasekhar(1960).

We have written the line source functions for the Stokes parameters I and Q in a suitable form and solved the Eq.(1) for

I_l and I_r . We find that due to the assumption of complete redistribution mechanism, the angular phase matrix is not affected by the velocity field and the velocity field affects only the frequency dependence of the absorption and re-emission profiles, as in non-polarized cases. If we were to consider partial redistribution mechanism, the angle dependent redistribution functions would have been affected by the velocity field and there would have been an inextricable coupling between the angles and frequencies. We have chosen azimuthally independent incident radiation field with Rayleigh phase function. All these lead to axi-symmetric situations. In passing, one should mention that we have not considered the time dependent radiative transfer equation because the period of the wave is much larger than the mean time necessary for a photon to escape the atmosphere. Therefore we could solve the transfer equation at different time steps independently.

We modified the Discrete space theory technique of Grant & Hunt(1969a) to solve the vector transfer equation. Stability and accuracy of this method for plane parallel medium has been discussed by Grant and Hunt (1969b). Use of this basic technique to solve the transfer equation with spherical symmetry has been described by Peraiah and Grant (1973). But in this paper we are concerned with only plane parallel medium and sinusoidal velocity input. Therefore a brief description of the method is given in the Appendix.

2.1. Numerical checks employed

First we checked the flux conservation for a purely scattering medium. We considered 25 and 31 frequency points in the domain [-6,6]. They refer to two different frequency mesh sizes. The results for 25 frequency points and 31 frequency points do not differ much. The error is less than 1%. This means that our choice of the frequency mesh size is sufficient. Next we extended the frequency domain to [-8,8] with 33 frequency points. Again the intensity and polarization results do not differ within the frequency points [-6,6]. We have assumed only the complete redistribution mechanism which is valid in the Doppler core and our choice may be just adequate. In the static cases, the Doppler core extends from -3 to +3 Doppler widths. Since we have the presence of acoustic wave with a 3 Doppler width amplitude, we should perform the calculations to cover [-6,6] frequency range. By choosing the same velocity and atmospheric model as that of Scharmer (1984), and obtaining the same results for the specific intensity, we ensured the accuracy of our calculations in the presence of a damped acoustic wave. We (Mohan Rao and Rangarajan, 1993) have already checked the correctness of the calculation of polarization for a static atmosphere obtained by this code by comparing with the results of Faurobert (1987). She had used Feutrier technique to solve the problem. We tried two different angular mesh sizes. We employed 3 and 4 angle Gaussian quadrature to take care of the scattering integral. We find a difference of nearly 20% (error) between these two different mesh sizes at very few frequency points. This error analysis was performed for only at one particular time step and it shows both higher and lower values for the 3 angle case compared to the

four angle case. Therefore on an average, over the whole period of the wave, the lesser mesh size may not give much error. The discrete space theory method has the advantage of flexibility. If we want to introduce some more physical processes, the 'extra' terms will change only the 'cell' matrices and the basic structure of the algorithm remains the same. It is quite accurate and stable too. But it is computationally expensive since the matrix sizes go up if we increase the number of frequencies or angles, and a lot of inversion of matrices need to be done. A typical matrix size is given by: number of frequency points \times number of angles \times number of polarization states. In each layer one has to calculate two reflection and two transmission matrices. For this problem, one can perform the calculations for each time step separately which reduces the burden on the main memory. We required 64 MB of main memory to handle this problem and it takes two hours of CPU time on DEC Alpha workstation to calculate the profiles at one time step.

A new technique to handle polarized radiative transfer based on perturbation methods may be faster and better suited to certain class of problems (Faurobert et al. 1996). At present we have not made any comparison between our method and that of Faurobert et. al. (1996).

3. Results and discussion

The atmospheric parameters were chosen to represent very roughly the conditions of formation of Ca II K line in a chromosphere. We took $\beta_c = 10^{-7}$, $\epsilon = 10^{-4}$ and a depth independent damping parameter $a = 10^{-3}$. The planck function B appearing in Eq.(7) was varied with depth according to

$$B(\tau_c) = 1 + 10\tau_c^{0.9} + 100\exp(-70.7\sqrt{\tau_c}). \quad (9)$$

which gives temperature minimum near at $\tau_c = 10^{-2}$. Here τ_c refers to the continuum optical depth. We have used the number of angular points $n_\mu = 3$, and the number of depth points to be $n_\tau = 48$, covering the range $10^{-11} < \tau_c < 10$. The choice of the above parameters are from Scharmer (1984). We dealt with three different types of waves and they are described below.

3.1. Damped sine wave

The vertical velocity of the wave was assumed to be of the form,

$$v = v' \sin\phi', \quad (10)$$

where the amplitude v' was written as

$$v' = v_0/[1 + \sqrt{\tau_c/\tau^*}] \quad (11)$$

and τ^* is roughly the depth where v' saturates to v_0 . The phase ϕ' is given by

$$\phi' = 2\pi(z - ct)/cP. \quad (12)$$

Here z is the height, t is the time and P the period of the wave. This form of the velocity simulates the growth of the amplitude

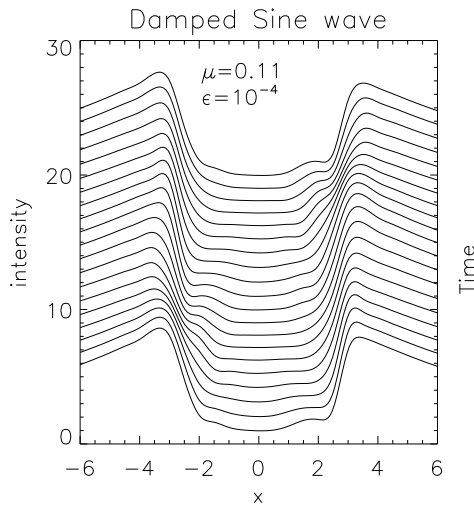


Fig. 1a. Time evolution of the specific intensity

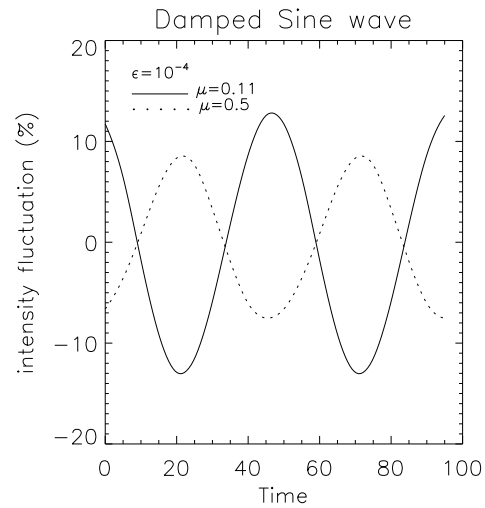


Fig. 2a. Fluctuation of the intensity at the line center

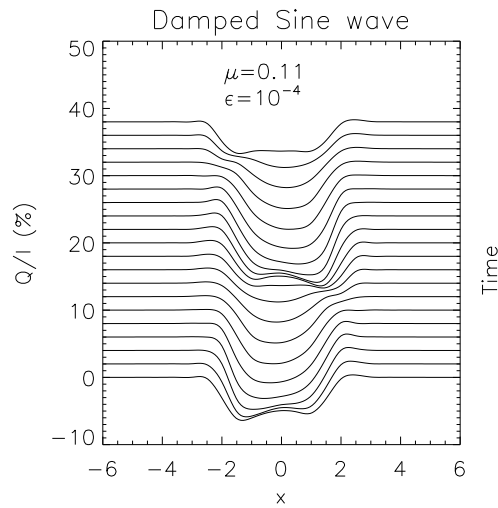


Fig. 1b. Time evolution of the polarization

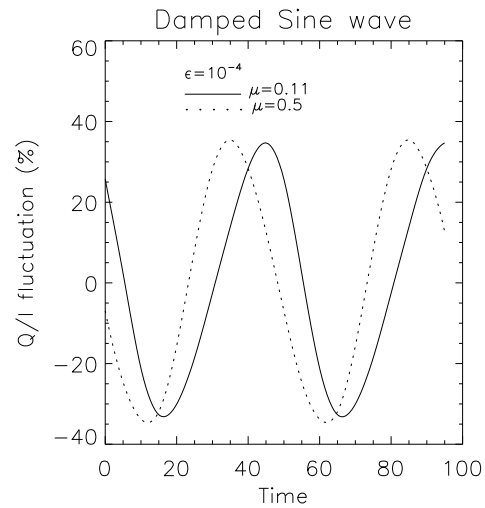


Fig. 2b. Fluctuation of the polarization at the line center

of a damped adiabatic acoustic wave in an isothermal atmosphere. This wave model is chosen from Scharmer (1984). We chose the period P to be 100 sec, $\tau^* = 10^{-3}$, $c = 7\text{km s}^{-1}$ and $v_0 = 3\text{km s}^{-1}$. The amplitude of the wave is 3 Doppler units.

The time resolution of our calculations is 5 secs. In Fig. 1a and b, we have plotted the time evolution of the intensity and the polarization in the direction $\mu = 0.11$ (limb direction) with respect to the frequency x . The profiles are shifted in the y-axis by a constant amount so that they can be perceived. Therefore the ordinate values for only the bottom most curve can be directly read. We have not plotted the result for $\mu = 0.89$ because the polarization is the least in that direction and zero at $\mu = 1.0$. One can clearly see the effect of the wave by the distortion it has produced on the profile shape. Here it is not as dramatic as in the case of Scharmer (Fig. 4c, 1984) because he has plotted at $\mu = 0.89$ in the direction of which the effect is maximum. But we find that the polarization shows the effect of the wave

better than the intensity. The change in the shape can be easily understood as being due to the change in optical depth brought about by the Doppler shift through the profile function.

The intensity and the polarization fluctuations as a function of time at the line center are shown in Fig. 2a and b for two different ray directions. If we define the intensity fluctuation as

$$fluctuation = \frac{I_{av}(\mu) - I(t, \mu)}{I_{av}(\mu)}$$

we find that this quantity is symmetric with respect to the mean. The figure shows that the intensity and polarization fluctuate with a period which is nearly half of that of the wave. An excellent reasoning for this phenomenon is already given by Scharmer and so we will not repeat it here. But we note that both the intensity and the polarization show some phase difference between the two directions due to the path difference. We can also see that the amplitude of the intensity fluctuations is less than that of the polarization. Polarization is a measure of

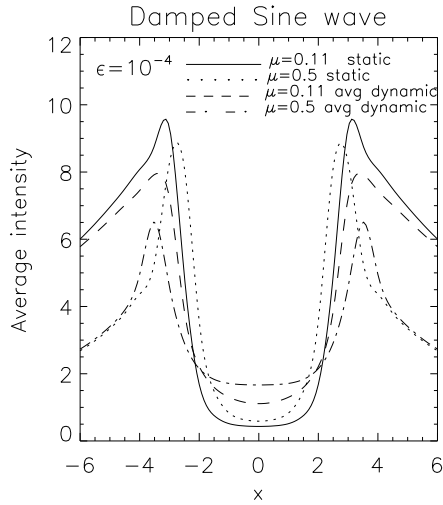


Fig. 3a. Time average of the intensity over one full period

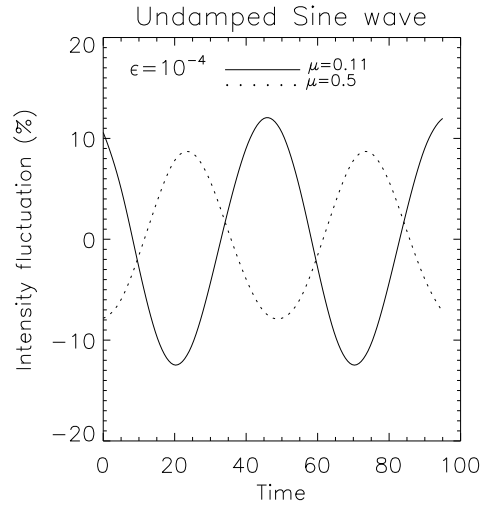


Fig. 4a. Same as Fig. 2a

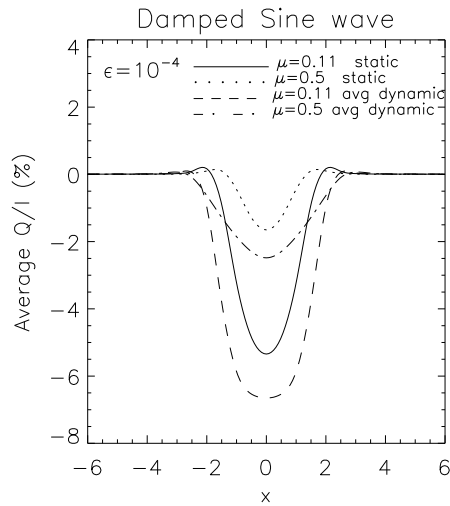


Fig. 3b. Time average of the polarization over one full period

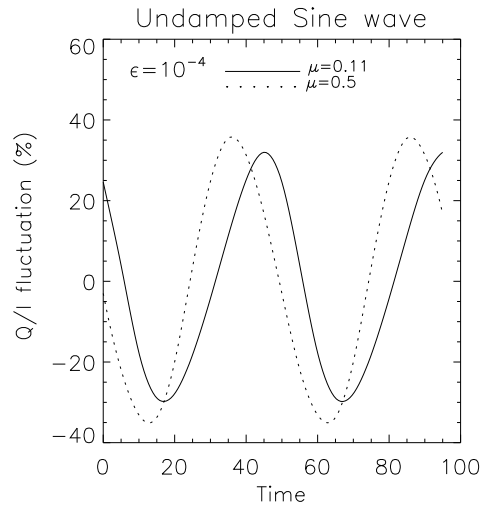


Fig. 4b. Same as Fig. 2b

anisotropy. The absorption coefficient is affected by the velocity in different directions by different amounts thereby aiding the anisotropy in the radiation field. This may be a motivation for looking for the polarization changes while studying the wave phenomenon in the limb direction.

The time averaged intensity and polarization profiles in two different directions are plotted in Fig. 3a and b. We have also shown the static profiles with the same atmospheric structure for the comparison sake. We find that the line center intensity is enhanced by a factor of nearly three for the dynamic model compared to the static one irrespective of the direction. The average polarization becomes zero in the line wings and this is due to the assumption of complete redistribution mechanism.

We wish to acknowledge the fact that this is not a good assumption for studying the wing polarization of strong resonance lines as already noted by several authors and we hope to correct this inadequacy in our future work. The partial re-

distribution mechanism might have brought out the interesting interplay between the wave motion and the resonance line scattering. Nevertheless our work is valid in the Doppler core.

3.2. Undamped sine wave

We considered $v' = v_0$, in Eq.(11) and made it as a constant throughout the atmosphere. This ensures a constant maximum amplitude for the velocity. Such a representation was discussed by Shine (1975). The velocity period and other terms were the same as before. The results are shown in figures 4 and 5. We find that neither the fluctuations nor the averages of the quantities are very much different from the case of damped sine wave which may be due to the following reasons. The magnitude of the velocity amplitude and the complete redistribution mechanism which we have chosen are quite effective only in the Doppler core. But the damping may affect only the wings to which our model is insensitive.

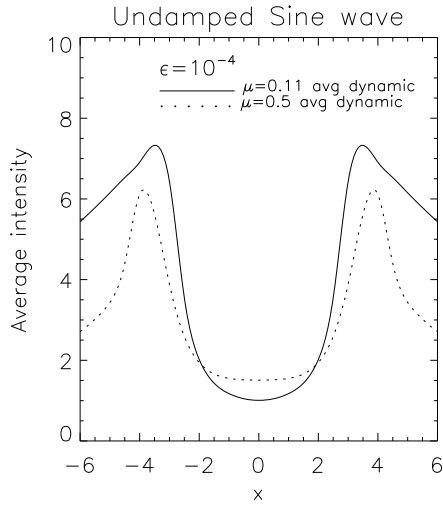


Fig. 5a. Same as Fig. 3a

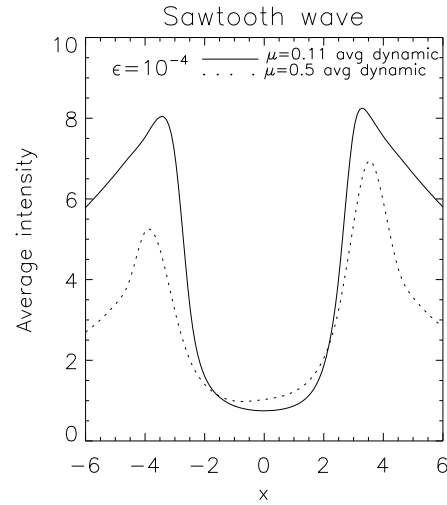


Fig. 6a. Same as Fig. 3a

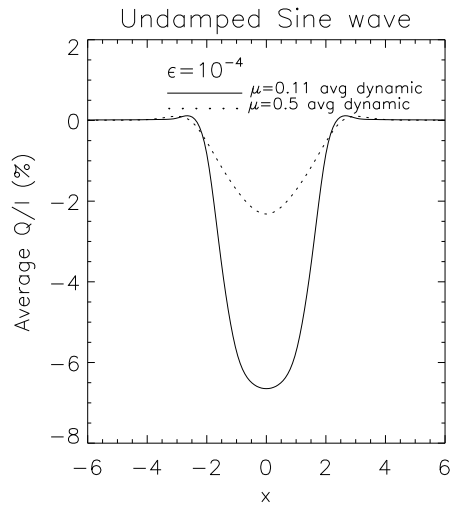


Fig. 5b. Same as Fig. 3b

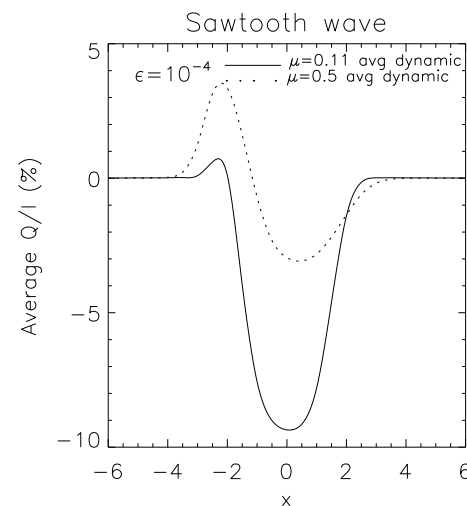


Fig. 6b. Same as Fig. 3b

3.3. Sawtooth wave

Following Shine (1975), we chose a sawtooth wave of the form

$$v = v_0 [2((z - ct)/cP)_{\text{mod } 1} - 1]. \quad (13)$$

Here the mod 1 indicates that only the excess above the next smallest integer of the enclosed quantity is used. The time averaged intensity and the polarization obtained with this representation of the velocity is shown in Fig. 6. The asymmetry in the average profile was already noticed by Shine (1975). But the polarization shows a noticeable flip of the sign within the profile in the averaged quantity in the direction $\mu = 0.5$. This may be due to a jump in the optical depth which must have made the medium optically thin at this frequency to give a 'positive' polarization.

We have also computed the profiles for the case of $\epsilon = 10^{-5}$ and velocity amplitude $v_0 = 1 \text{ km s}^{-1}$. Since we did not find significant differences for $\epsilon = 10^{-5}$ from that of $\epsilon = 10^{-4}$

cases, we have not included those results here. But for velocity amplitude $v_0 = 1$ we find the average intensity profile to be narrower compared to $v_0 = 3$ which is in agreement with that of Scharmer. Since the intensity for $v_0 = 1 \text{ km s}^{-1}$ is higher compared to $v_0 = 3 \text{ km s}^{-1}$ we find these cases show more polarization at line center. An extensive study of different waves with different amplitudes with partial redistribution formalism is underway and will be reported in future.

4. Conclusions

By this study we have shown that there is considerable difference in the resonance line polarization profiles from a dynamic atmosphere compared to the static one. If we use static model to interpret dynamic phenomena, we may miss many interesting effects. The same conclusion was arrived at by Carlsson and Stein (1995) by detailed modelling. Our results also show

that we can obtain additional information regarding the type of wave from the studies of resonance line polarization. Future work should include the PRD effects, a more realistic model atmosphere and so on. Observations may be planned to obtain the time resolved resonance line polarization.

Acknowledgements. The useful suggestions made and the clarifications sought by the unknown referee has improved the quality of the paper considerably and the author would like to thank the referee for that. I like to thank Prof.A.Peraiah and Prof. Ramnath Cowsik for the facilities they provided me and also their constant encouragement. I am grateful to Mr. B.A.Varghese for his help in making the figures shown in this paper. I would like to thank Dr.D.Mohan Rao for many suggestions. I also benefitted by my discussions with Prof.S.Hasan and P.Venkatakrisnan.

Appendix A: method of solution

A.1. Interaction principle

The Discrete Space Theory technique is based on interaction principle and the 'Star product' algorithm. These two ideas are described in great detail in Grant and Hunt (1969a). Interaction principle gives the relationship between the input and output radiation fields from a given medium. Consider the medium to be stratified into different layers z_1, z_2, \dots, z_N . At any layer we define two oppositely directed beams as $\mathbf{I}^+(z_n)$ and $\mathbf{I}^-(z_n)$. Let $\mathbf{I}^+(z_n)$ and $\mathbf{I}^-(z_{n+1})$ be the incident intensities. The emergent intensities from the layer depend on the incident intensities and on the sources $\sum^+(z_n, z_{n+1}), \sum^-(z_{n+1}, z_n)$ present within the layer. Thus we can write

$$\mathbf{I}^+(z_{n+1}) = t(z_{n+1}, z_n)\mathbf{I}^+(z_n) + r(z_n, z_{n+1})\mathbf{I}^-(z_{n+1}) + \sum^+(z_{n+1}, z_n), \quad (\text{A1})$$

$$\mathbf{I}^-(z_n) = r(z_{n+1}, z_n)\mathbf{I}^+(z_n) + t(z_n, z_{n+1})\mathbf{I}^-(z_{n+1}) + \sum^-(z_n, z_{n+1}), \quad (\text{A2})$$

or

$$\begin{pmatrix} \mathbf{I}_{n+1}^+ \\ \mathbf{I}_n^- \end{pmatrix} = S(n, n+1) \begin{pmatrix} \mathbf{I}_n^+ \\ \mathbf{I}_{n+1}^- \end{pmatrix} + \sum(n, n+1). \quad (\text{A3})$$

The linear operators $t(n, n+1), t(n+1, n), r(n+1, n), r(n, n+1)$ of which the first two are operators of diffuse transmission and the last two are for diffuse reflexion. They include the geometry and the physical properties of the medium. Once we obtain the response functions for a layer of specified boundaries with given inputs, we can proceed to calculate the response functions for two or more consecutive layers by a process termed as 'Star product'.

A.2. Derivation of reflection and transmission matrices for a single layer for the case of polarized line transfer with complete redistribution mechanism

Rewriting the Eq. (1) for the two oppositely directed beams and using some of the above definitions we get,

$$\pm \mu \frac{d\mathbf{I}(x, \pm \mu, z)}{dz} = k_L [\beta + \phi(x, \pm \mu)] [\mathbf{S}(x, \pm \mu, z) - \mathbf{I}(x, \pm \mu, z)]. \quad (\text{A4})$$

This problem can be solved by a suitable discretization in frequency, direction and space for both the polarization states. For the frequency discretization, we choose division points $\{\psi_i\}$ and weights $\{a_i\}$ such that

$$\int_{-\infty}^{\infty} f(\psi) d\psi \simeq \sum_{i=-m}^{i=m} a_i f(\psi_i) \quad (\text{A5})$$

and for the directional discretization we choose abscissae $\{\mu_j\}$ and weights $\{c_j\}$ such that

$$\int_0^1 f(\mu) d\mu \simeq \sum_{j=1}^J c_j f(\mu_j). \quad (\text{A6})$$

We define the $J \times J$ matrices

$$\mathbf{c} = [c_j \delta_{ij}] \quad \mathbf{M}_J = [\mu_j \delta_{ij}] \quad (\text{A7})$$

where c_j 's and μ_j 's are the weights and roots of Gauss - Legendre angular quadrature of the order J in the interval (0, 1). In the 'cell' method of deriving difference equations one formally integrates Eq. (12) over an interval $[z_n, z_{n+1}] \times [\mu_{j-\frac{1}{2}}, \mu_{j+\frac{1}{2}}]$ defined on a two dimensional grid. Using the definition of optical depth, one obtains,

$$\begin{aligned} \mathbf{M}_m(\mathbf{I}_{i,n+1}^+ - \mathbf{I}_{i,n}^+) + \tau_{n+\frac{1}{2}}(\beta + \phi_i^+)_{n+\frac{1}{2}} \mathbf{I}_{i,n+\frac{1}{2}}^+ \\ = \tau_{n+\frac{1}{2}}(\beta + \epsilon \phi_i^+)_{n+\frac{1}{2}} \mathbf{B}_{n+\frac{1}{2}} \\ + \frac{1}{2} \tau_{n+\frac{1}{2}} \sigma_{n+\frac{1}{2}} \sum_{i'=-m}^m a_{i',n+\frac{1}{2}} \mathbf{c} \\ [\phi^+ \mathbf{P} \mathbf{I}^+ + \phi^- \mathbf{P} \mathbf{I}^-]_{i',n+\frac{1}{2}} \end{aligned} \quad (\text{A8})$$

and

$$\begin{aligned} \mathbf{M}_m(\mathbf{I}_{i,n}^- - \mathbf{I}_{i,n+1}^-) + \tau_{n+\frac{1}{2}}(\beta + \phi_i^-)_{n+\frac{1}{2}} \mathbf{I}_{i,n+\frac{1}{2}}^- \\ = \tau_{n+\frac{1}{2}}(\beta + \epsilon \phi_i^-)_{n+\frac{1}{2}} \mathbf{B}_{n+\frac{1}{2}} \\ + \frac{1}{2} \tau_{n+\frac{1}{2}} \sigma_{n+\frac{1}{2}} \sum_{i'=-m}^m a_{i',n+\frac{1}{2}} \mathbf{c} \\ [\phi^+ \mathbf{P} \mathbf{I}^+ + \phi^- \mathbf{P} \mathbf{I}^-]_{i',n+\frac{1}{2}}. \end{aligned} \quad (\text{A9})$$

Here $(n + \frac{1}{2})$ denote averages for the layer and $\sigma_{n+\frac{1}{2}} = 1 - \epsilon_{n+\frac{1}{2}}$. The vectors are defined as

$$\mathbf{I}_{i,n}^{\pm} = \begin{pmatrix} I(\pm \mu_1, \psi_i; \tau_n) \\ I(\pm \mu_2, \psi_i; \tau_n) \\ \vdots \\ I(\pm \mu_J, \psi_i; \tau_n) \end{pmatrix} \quad (\text{A10})$$

$$\phi_{i,n+\frac{1}{2}}^{\pm} = \begin{pmatrix} \phi(x_i, \pm\mu_1, \tau_{n+\frac{1}{2}}) \\ \phi(x_i, \pm\mu_2, \tau_{n+\frac{1}{2}}) \\ \vdots \\ \phi(x_i, \pm\mu_J, \tau_{n+\frac{1}{2}}) \end{pmatrix}.$$

Corresponding to each pair of subscripts (i, j) , we now define an index k so that

$$(i, j) \equiv k = j + (i - 1)J, \quad 1 \leq k \leq K = mJ. \quad (A11)$$

We extend this K vectors to $2K$ vectors to take into account of two polarization states. Let $\phi_{n+\frac{1}{2}}^{\pm}$ and $S_{n+\frac{1}{2}}^{\pm}$ be $2K$ vectors where the first K elements of $S_{n+\frac{1}{2}}^{\pm}$ are defined by

$$S_{k,n+\frac{1}{2}}^{\pm} = (\beta + \epsilon\phi_k^{\pm})_{n+\frac{1}{2}} B_{n+\frac{1}{2}} \quad (A12)$$

and they are repeated for the next K elements. Similarly, let Φ and \mathbf{M} be $2K \times 2K$ matrices defined by

$$\Phi_{n+\frac{1}{2}}^{\pm} = [(\beta + \phi_k^{\pm})_{n+\frac{1}{2}} \delta_{kk'}]$$

$$\mathbf{M} = \begin{pmatrix} \mathbf{M}_J & & & \\ & \mathbf{M}_J & & \\ & & \ddots & \\ & & & \mathbf{M}_J \end{pmatrix},$$

and \mathbf{P}_R is also extended to include the frequencies as a \mathbf{P} matrix. Using the linear interpolation scheme,

$$\frac{\mathbf{I}_n^{\pm} + \mathbf{I}_{n+1}^{\pm}}{2} = \mathbf{I}_{n+\frac{1}{2}}^{\pm} \quad (A13)$$

we obtain

$$\left(\mathbf{M} + \frac{\tau}{2}\mathbf{Z}^+\right)\mathbf{I}_{n+1}^+ - \frac{\tau}{2}\mathbf{Y}^-\mathbf{I}_n^- = \left(\mathbf{M} - \frac{\tau}{2}\mathbf{Z}^+\right)\mathbf{I}_n^+ + \frac{\tau}{2}\mathbf{Y}^-\mathbf{I}_{n+1}^- + S^+ \quad (A14)$$

$$\left(\mathbf{M} + \frac{\tau}{2}\mathbf{Z}^-\right)\mathbf{I}_n^- - \frac{\tau}{2}\mathbf{Y}^+\mathbf{I}_{n+1}^+ = \left(\mathbf{M} - \frac{\tau}{2}\mathbf{Z}^-\right)\mathbf{I}_{n+1}^- + \frac{\tau}{2}\mathbf{Y}^+\mathbf{I}_n^+ + S^- \quad (A15)$$

where

$$\mathbf{Z}^+ = \Phi^+ - \frac{\sigma}{2}\phi^+(\phi^+)^T \mathbf{acP}, \quad \mathbf{Z}^- = \Phi^- - \frac{\sigma}{2}\phi^-(\phi^-)^T \mathbf{acP},$$

$$\mathbf{Y}^+ = \frac{\sigma}{2}\phi^+(\phi^-)^T \mathbf{acP}, \quad \mathbf{Y}^- = \frac{\sigma}{2}\phi^-(\phi^+)^T \mathbf{acP},$$

$$\Delta^+ = [\mathbf{M} + \frac{\tau}{2}\mathbf{Z}^+]^{-1}, \quad \Delta^- = [\mathbf{M} + \frac{\tau}{2}\mathbf{Z}^-]^{-1},$$

$$\mathbf{r}^{+-} = \frac{\tau}{2}\Delta^+\mathbf{Y}^-, \quad \mathbf{r}^{-+} = \frac{\tau}{2}\Delta^-\mathbf{Y}^+,$$

$$\mathbf{R}^{+-} = [\mathbf{I} - \mathbf{r}^{+-}\mathbf{r}^{-+}]^{-1}, \quad \mathbf{R}^{-+} = [\mathbf{I} - \mathbf{r}^{-+}\mathbf{r}^{+-}]^{-1},$$

$$\mathbf{A} = \mathbf{M} - \frac{\tau}{2}\mathbf{Z}^+, \quad \mathbf{D} = \mathbf{M} - \frac{\tau}{2}\mathbf{Z}^-.$$

Here \mathbf{I} is the identity matrix. Using the above definitions and the equations we can write the transmission and reflection matrices for a single layer as,

$$T(n+1, n) = \mathbf{R}^{+-}[\Delta^+\mathbf{A} + \mathbf{r}^{+-}\mathbf{r}^{-+}]$$

$$T(n, n+1) = \mathbf{R}^{-+}[\Delta^-\mathbf{D} + \mathbf{r}^{-+}\mathbf{r}^{+-}]$$

$$R(n+1, n) = \mathbf{R}^{-+}\mathbf{r}^{-+}[\mathbf{I} + \Delta^+\mathbf{A}]$$

$$R(n, n+1) = \mathbf{R}^{+-}\mathbf{r}^{+-}[\mathbf{I} + \Delta^-\mathbf{D}]$$

and the cell source vectors as,

$$\sum^+ = \mathbf{R}^{+-}[\Delta^+S^+ + \mathbf{r}^{+-}\Delta^-S^-]\tau$$

$$\sum^- = \mathbf{R}^{-+}[\Delta^-S^- + \mathbf{r}^{-+}\Delta^+S^+]\tau.$$

By making use of the boundary conditions and the star algorithm, one can build the response functions for the entire medium to solve for the output radiation field (see Peraiah, 1978). Recently Mohan Rao et.al (1995) have shown that this algorithm is stable against logarithmic step size for the layers.

References

- Carlsson M., Stein R.F., 1995, ApJ 440 L29
 Chandrasekhar S., 1960, Radiative Transfer, Oxford University Press, Dover
 Cram L.E., 1972, Sol.Phys. 22, 375
 Deubner, F.-L., 1991, Mechanisms of Chromospheric and Coronal Heating In: Ulmschneider P., Priest E.R., Rosner R. (eds.) Observations of waves and oscillations, Berlin: Springer-Verlag, p.6
 Dumont, S., Omont, A., Pecker, J.C., 1973, Sol.Phys. 28, 271
 Faurobert M., 1987, A&A 178, 269
 Faurobert-Scholl M., 1992, A&A 258, 521
 Faurobert-Scholl M., 1995, A&A 298, 289
 Faurobert M., Frisch H., Nagendra K.N., 1996, Submitted to A&A.
 Grant I.P., Hunt G.E., 1969a, Proc.R.Soc.London A 313, 183
 Grant I.P., Hunt G.E., 1969b, Proc.R.Soc.London A 313, 199
 Grant I.P., Peraiah A., 1972, MNRAS 160, 239
 Heasley J.N., 1975, Sol.Phys. 44, 275
 Mihalas D., 1978, Stellar Atmospheres 2nd edn., Freeman, San Francisco
 Mohan Rao D., Rangarajan K.E., 1993, A&A 274, 993
 Mohan Rao D., Varghese B.A., Srinivasa Rao M., 1995, JQSRT 53, 639
 Peraiah A., 1978, Kodaikanal Obs. Bull Ser. A 2, 115
 Rammacher W., Ulmschneider P., 1992, A&A 253, 583
 Redman R.O., 1941, MNRAS 101, 266
 Rees D.E., Saliba G., 1982, A&A 115, 1.
 Scharmer G.B., 1984, Methods in Radiative Transfer In: Kalkofen W. (ed) Accurate solutions to Non-LTE problems using approximate Lambda operators, Cambridge University Press, p.173
 Scharmer G.B., Nordlund A., 1982 Stockholm Obs. Report 19
 Shine R.A., 1975, ApJ 202, 543
 Solanki S.K., Roberts B., 1992, MNRAS 256, 13
 Stenflo J.O., Twerenbold D., Harvey J.W., 1983a, A&AS 52, 161
 Stenflo J.O., Twerenbold D., Harvey J.W., Brault J.W., 1983b, A&AS 54, 505
 Stenflo J.O., 1994, Solar Magnetic Fields, Kluwer Academic Publishers, Dordrecht